

Article

Research on the Influence of Tractor Parameters on Shift Quality, Based on Uniform Design

Junyan Wang^{1,2}, Changgao Xia^{1,*}, Xin Fan^{1,3} and Junyu Cai¹

¹ School of Automotive and Traffic Engineering, Jiangsu University, Zhenjiang 212013, China; wangjy@zjc.edu.cn (J.W.); aming@jsut.edu.cn (X.F.); 2111504010@stmail.ujs.edu.cn (J.C.)

² School of Transportation, Zhenjiang College, Zhenjiang 212028, China

³ School of Automobile and Traffic Engineering, Jiangsu University of Technology, Changzhou 213001, China

* Correspondence: xiagc@ujs.edu.cn; Tel.: +86-138-1517-1208

Abstract: This paper mainly studies the influence of tractor parameters on shift quality. The kinetic theoretical model of the powertrain system was deduced, and then the simulation model was established by using AMESim simulation software. The acceptable jerk and shift time were selected as the evaluation indexes of shift quality. The influence of engine speed, the tractive resistance of the tractor, the clutch oil pressure and the orifice diameter on the above evaluation indexes were quantitatively studied. The simulation test, under the influence of a single parameter, was carried out using the parameter analysis method. After this, the uniform design experimentation method was used to carry out the simulation test, under the influence of combined parameters. The results showed that in order to improve the shift quality, it is necessary to focus on the selection of clutch oil pressure and orifice diameter.

Keywords: shift quality; hydro-mechanical continuously variable transmission; proportional pressure reducing valve; AMESim; uniform design



Citation: Wang, J.; Xia, C.; Fan, X.; Cai, J. Research on the Influence of Tractor Parameters on Shift Quality, Based on Uniform Design. *Appl. Sci.* **2022**, *12*, 4895. <https://doi.org/10.3390/app12104895>

Academic Editor: Stephanos Theodossiades

Received: 9 April 2022

Accepted: 9 May 2022

Published: 12 May 2022

Publisher's Note: MDPI stays neutral with regard to jurisdictional claims in published maps and institutional affiliations.



Copyright: © 2022 by the authors. Licensee MDPI, Basel, Switzerland. This article is an open access article distributed under the terms and conditions of the Creative Commons Attribution (CC BY) license (<https://creativecommons.org/licenses/by/4.0/>).

1. Introduction

In recent years, hydro-mechanical continuously variable transmission (HMCVT) has been widely studied [1–3]. It not only uses hydraulic static transmission to realize stepless speed regulation, but also relies on mechanical transmission parts to improve transmission efficiency [4–6]. Although a tractor equipped with a front-end loader can achieve stepless speed change by matching the HMCVT described above, it is inevitable that the driver needs to operate and change the working direction frequently. This can make the driver uncomfortable and shorten the service life of the clutch in the transmission [7]. To overcome these drawbacks, in this study the HMCVT was combined with two multi-plate wet clutch assemblies to achieve fast commutation movements of the tractor powertrain [8]. The system methodology was used to model and simulate the power reversing system of an agricultural tractor [9]. For a long time, the research of fast power reversing transmission systems or HMCVT focused on the structure design and performance analysis [10–13]. A continuously variable transmission scheme with fast power reversing was proposed, and the transmission characteristics of the transmission scheme were studied theoretically and verified by a simulation [14]. With the increasing requirements for tractor smoothness, the study of dynamic characteristics of shift quality has become a key research focus.

In previous research on this topic [15], the effects of the design parameters of a power shuttle tractor on the shift performance have been investigated using simulations. The shift performance was evaluated in terms of the peak torques of the input shaft and the tractor axles, the power transmitted per unit area of the clutch, and in terms of the time required to transmit the power. This research only investigated the effect of a single design parameter on the evaluation index. Furthermore, previous research [16] has also studied the shift quality of a tractor in the acceleration phase. The shift quality was evaluated by

the peak acceleration of the tractor and the frictional work of the clutch. Moreover, [17] other research has also reported that the shift quality was improved by controlling the clutch current profile, and that the relative amplitude of jerk was used to decide the regular shift performance. However, the indexes chosen by the above-mentioned studies to assess shift quality were all transient indicators and did not take into account the time course of the jerk. In addition, these studies [15,16] did not consider the effect of combined design parameters on the shift quality, which is far from the actual engineering situation. The orthogonal test method was widely used to study the influence of combined parameters on the shift quality [18,19]. However, this method is less suitable for applications with a large range of parameter values and many factor levels (greater than five).

Accordingly, this paper has selected acceptable jerk and shift time as the evaluation indexes of tractor shift quality. These indexes comprehensively considered the influence of the peak jerk and its continuous impact in the shift process. The uniform design experimentation method was used to carry out the simulation test, under the influence of combined parameters, and the interaction between these parameters was also taken into account. Moreover, the kinetic model was established according to the structure of the powertrain, and then the simulation model was established based on AMESim software. A research method based on simulation could simplify the research and development process of HMCVT. It could also provide the basis for follow-up research and development and help to avoid a variety of possible problems.

2. Powertrain Model

2.1. HMCVT Mechanical System

The HMCVT is shown as a stick diagram in Figure 1. As can be seen, the engine and the HMCVT were connected by an input shaft. The structure of the HMCVT was mainly composed of the following four parts: a variable displacement pump-fixed displacement motor system (pump-motor), a planetary gear mechanism (PGM), shifting clutches (C1, C2, C3, and C4), and directional clutches (CF and CR).

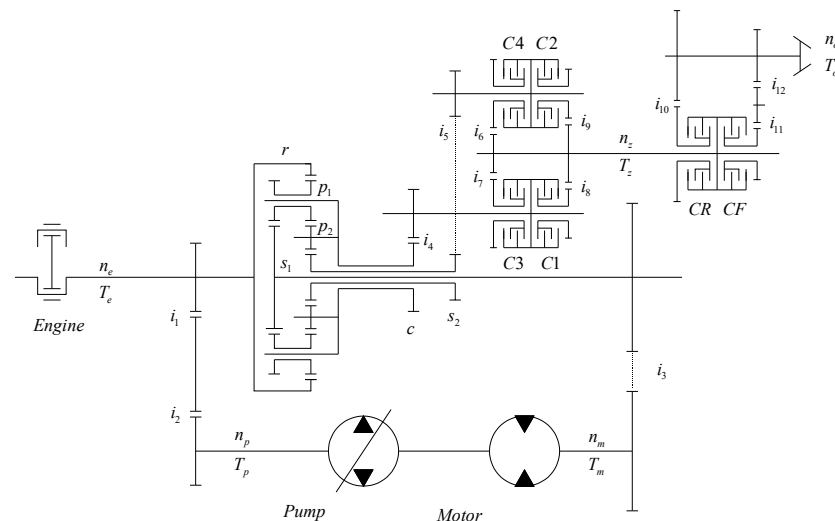


Figure 1. HMCVT stick diagram.

Table 1 shows the clutches' engagement schedule and the gearbox and rear axle gear ratios. Please note, that only forward driving conditions were considered in this paper, and reverse driving conditions were not considered.

Table 1. Clutches’ engagement schedule for the HMCVT.

Range		Directional Clutch		Shifting Clutch				Gearbox Gear Ratio (INPUT to Output Shaft)	Rear Axle Gear Ratio
		CF	CR	C1	C2	C3	C4		
Forward	First	+		+				8.62~4.59	20.72
	Second	+			+			4.59~2.43	
	Third	+				+		2.43~1.30	
	Fourth	+					+	1.30~0.69	

2.1.1. Rotational Dynamics of the HMCVT

To capture the low frequency dynamic effects that result from events such as gear shifting and clutch selection, an HMCVT model with lumped inertias was considered. A schematic of the aforementioned HMCVT is shown in Figure 2.

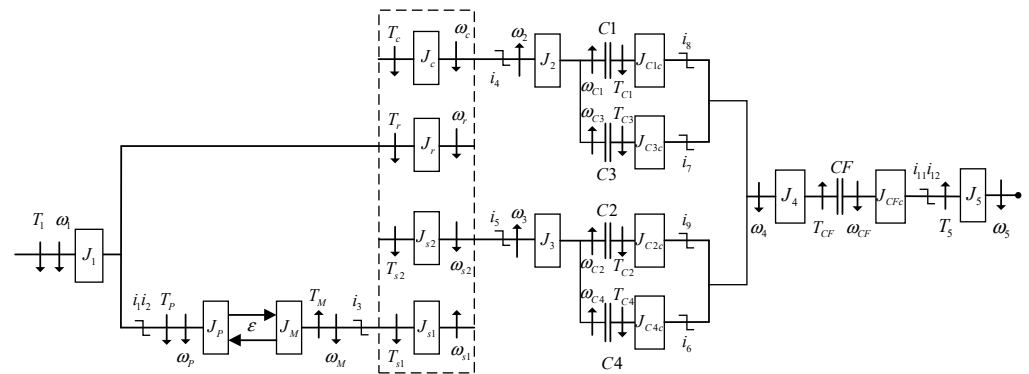


Figure 2. Rotational dynamics of HMCVT.

By applying Newton’s second law for rotation at each of the inertias, the following set of equations, describing the rotational dynamics of the HMCVT mechanical system was obtained:

$$\text{Shaft 1 : } J_1 \frac{d\omega_1}{dt} = T_1 - T_r - \frac{T_P}{i_1 i_2} \tag{1}$$

$$\text{Shaft 2 : } J_2 \frac{d\omega_2}{dt} = i_4 T_c - T_{C1} - T_{C3} \tag{2}$$

$$\text{Shaft 3 : } J_3 \frac{d\omega_3}{dt} = i_5 T_{s2} - T_{C2} - T_{C4} \tag{3}$$

$$\text{Shaft 4 : } J_4 \frac{d\omega_4}{dt} = i_8 T_{C1} + i_9 T_{C2} + i_7 T_{C3} + i_6 T_{C4} - T_{CF} \tag{4}$$

$$\text{Shaft 5 : } J_5 \frac{d\omega_5}{dt} = i_{11} i_{12} T_{CF} - T_5 \tag{5}$$

$$\text{Large sun gear : } J_{s1} \frac{d\omega_{s1}}{dt} = i_3 T_M - T_{s1} \tag{6}$$

$$\text{Small sun gear : } J_{s2} \frac{d\omega_{s2}}{dt} = T_{s2} - \frac{T_{C2}}{i_5} - \frac{T_{C4}}{i_5} \tag{7}$$

$$\text{Ring gear : } J_r \frac{d\omega_r}{dt} = T_1 - \frac{T_P}{i_1 i_2} - T_r \tag{8}$$

$$\text{Carrier : } J_c \frac{d\omega_c}{dt} = T_c - \frac{T_{C1}}{i_4} - \frac{T_{C3}}{i_4} \tag{9}$$

where J is lumped inertia, $\text{kg}\cdot\text{m}^2$; ω is angular velocity, rad/s ; T is torque, Nm ; $i_1 \sim i_{12}$ are gear ratios; the subscripts C1, C2, C3, C4, and CF denote the clutches; and the subscripts P and M denote the pump and motor, respectively.

2.1.2. Variable Displacement Pump-Fixed Displacement Motor System

Ignoring the influence of internal and external leakage and the internal resistance of the pump motor system, the simplified kinetic model is as follows:

$$\frac{V_1}{\beta} \frac{dp_1}{dt} = D_P \varepsilon \omega_P - D_M \omega_M \tag{10}$$

$$J_P \frac{d\omega_P}{dt} = T_P - D_P \varepsilon (p_1 - p_2) \tag{11}$$

$$J_M \frac{d\omega_M}{dt} = D_M (p_1 - p_2) - T_M \tag{12}$$

where p_1 and p_2 denote the high and low side pressure values of the system, respectively, Pa; p_2 is equal to constant makeup pressure; V_1 is the volume of fluid on the high pressure side, m^3 , V_1 is equal to the sum of the volume of pump and motor oil cavity and the volume of the pipeline; β is the oil bulk modulus, Pa; and ε is the swash value, $-1 \leq \varepsilon \leq 1$.

2.1.3. Dynamic Clutch Friction Model

In this paper, we used the reset-integrator friction model, considering the Stribeck effect [20]. The effect of viscous friction was ignored, so the friction torque evolved smoothly, according to the equation below:

$$T_{dry} = T_{dyn} + (T_{stat} - T_{dyn}) \cdot e^{\left[\frac{-3|\omega_{rel}|}{astrib}\right]} \tag{13}$$

where $astrib$ is the Stribeck constant (positive value), r/min; T_{dyn} is the maximum transmittable torque during sliding, Nm; T_{stat} is the maximum transmittable torque during stiction, Nm; and ω_{rel} is the relative velocity, rad/s.

2.2. Longitudinal Tractor Dynamics

By ignoring tire slip, the tractor was simplified as a rigid body, with a mass of m_t . The resulting tractor dynamics were described by the following:

$$m_t R_{wr}^2 \frac{d\omega_{wr}}{dt} = T_{wr} - T_{tr} - 4T_{brake} \tag{14}$$

where R_{wr} is the radius of the driving wheel, m; ω_{wr} is the speed of the driving wheel, rad/s; T_{wr} is the driving wheel torque, Nm; T_{tr} is the road load torque, Nm; and T_{brake} is the wheel braking torque, Nm.

The parameters used in the simulation of the HMCVT mechanical system and the tractor are summarized in Table 2.

Table 2. Parameters used in simulation of the HMCVT mechanical system and the tractor.

Parameter	Value	Parameter	Value
J_1 (kg·m ²)	0.1283	J_2 (kg·m ²)	0.2940
J_3 (kg·m ²)	0.0940	J_4 (kg·m ²)	0.2500
J_5 (kg·m ²)	4.2333	J_{s1} (kg·m ²)	0.0022
J_{s2} (kg·m ²)	0.0040	J_r (kg·m ²)	0.0619
J_c (kg·m ²)	0.1893	$i_1 i_2$	1
i_3	-1.5	i_4, i_5	-2
i_6	-0.825	i_7	-0.580
i_8	-2.046	i_9	-2.920
$i_{11} i_{12}$	1	β (Pa)	1.7×10^9
V_1 (m ³)	6×10^{-4}	D_M (cm ³ /r)	54.8
D_P (cm ³ /r)	54.8	J_M (kg·m ²)	0.0520
J_P (kg·m ²)	0.0060	m_t (kg)	12,000
$astrib$ (r/min)	0.1	R_{wr} (m)	0.858

2.3. Hydraulic Component Actuation

The hydraulic actuation system significantly affected the operation of the HMCVT, a mathematical model of the hydraulic actuation system was necessary [21]. The simplified hydraulic actuation system in this paper included a pressure regulation system, a clutch actuation system, and a clutch cooling and lubrication system, as shown in Figure 3.

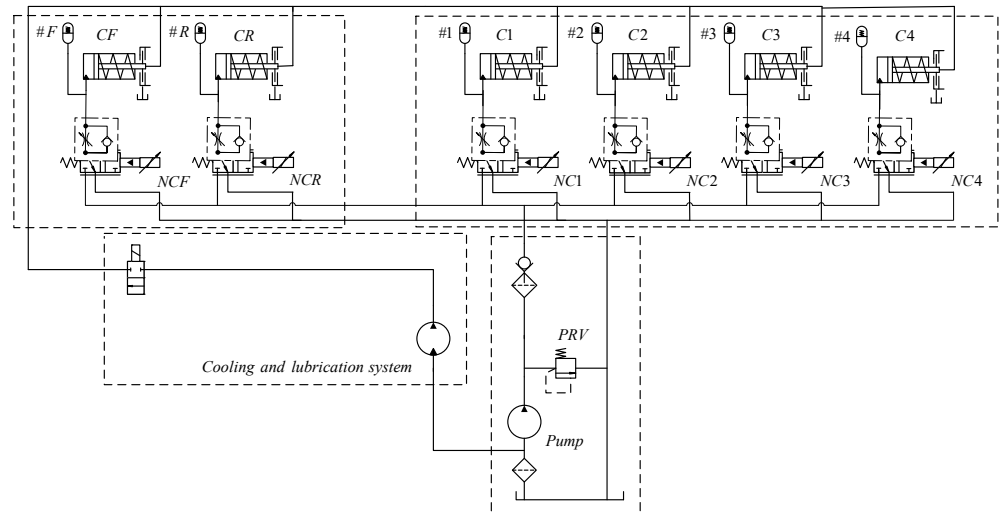


Figure 3. Simplified hydraulic actuation system.

2.3.1. Pressure Regulation System

The pump was powered by the engine, and supplies flowed to the hydraulic system at the volumetric flow rate, Q_{pump} , as follows:

$$Q_{pump} = D_{pump}\omega_e \tag{15}$$

where D_{pump} is the pump displacement, m^3/rad ; ω_e is the engine speed, rad/s . The volumetric flow rate through the pressure relief valve (PRV) was modeled as follows:

$$Q_{PRV} = \begin{cases} KV_{PRV}(P_{line} - P_{crack,PRV}) & \text{when } P_{line} > P_{crack,PRV} \\ 0 & \text{when } P_{line} \leq P_{crack,PRV} \end{cases} \tag{16}$$

where KV_{PRV} is the pressure relief valve gain, $m^3/s/Pa$; P_{line} is the line pressure, Pa ; and $P_{crack,PRV}$ is the cracking pressure, Pa .

2.3.2. Clutch Actuation System

The clutch actuation system consisted of six subsystems. Each system included a pilot-operated proportional pressure reducing valve ($NC1, NC2, NC3, NC4, NCF$ or NCR) and a clutch piston ($C1, C2, C3, C4, CF$ or CR). Thus, the $C1$ system shown in Figure 3 will be described in this section. The structure of the pilot-operated proportional pressure reducing valve, $NC1$, is shown in Figure 4.

Pilot-Operated Proportional Pressure Reducing Valve ($NC1$)

The mathematical model of $NC1$ consists of three subsystems. They are the spool mechanical system, the electromagnetic circuit, and the fluid flow system.

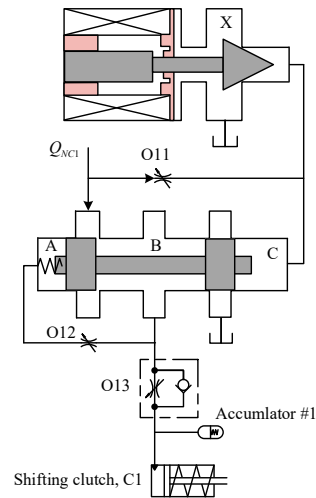


Figure 4. The structure of NC1.

(1) Spool mechanical systems

(a) Pilot valve

The pilot valve spool motion depended on the difference in pressure forces acting on the spool, the magnetic force, the inertia force, the viscous damping force, and the steady-state flow forces due to flow through the exhaust and inlet ports. The static friction force and the transient flow force were assumed to be negligible. Thus, the mechanical dynamics of the pilot valve were described by the following:

$$m_1 \cdot \frac{dx_1^2}{dt^2} + B_1 \frac{dx_1}{dt} = F_{mag,NC1} + F_{1,flow,NC1} - P_{NC1,X} A_{NC1,X} \quad (17)$$

where m_1 is the mass of the plunger, kg; B_1 is the viscous damping coefficient, N/(m/s); $F_{mag,NC1}$ is the magnetic force acting on the spool, N; $P_{NC1,X}$ is the pressure in chamber X, Pa; $A_{NC1,X}$ is the land cross-sectional areas at chamber X, m^2 ; x_1 is the spool displacement, m; and $F_{1,flow,NC1}$ is the net steady flow force acting on the spool, N.

(b) Main valve

The main valve spool motion depended on the difference in pressure forces acting on the spool, the net spring force, the inertia force, the viscous damping force, and the steady-state flow forces due to flow through the exhaust and inlet ports. The static friction force and the transient flow force were assumed to be negligible. Thus, the mechanical dynamics of the main valve were described by the following:

$$m_2 \frac{dx_2^2}{dt^2} + B_2 \frac{dx_2}{dt} + K_{NC1} x_2 = P_{NC1,C} A_{NC1,C} - P_{NC1,A} A_{NC1,A} - F_{2,flow,NC1} \quad (18)$$

where m_2 is the mass of the plunger, kg; B_2 is the viscous damping coefficient, Nm/rad/s; K_{NC1} is the spring constant, N/mm; $P_{NC1,A}$, $P_{NC1,C}$ are the pressures in chambers A and C, Pa; $A_{NC1,A}$, $A_{NC1,C}$ are the land cross-sectional areas at chambers A and C, m^2 ; x_2 is the spool displacement, m; and $F_{2,flow,NC1}$ is the net steady flow force acting on the spool, N.

(2) Electromagnetic circuit

In the range of the proportional electromagnetic force displacement characteristics, the output force equation of the proportional electromagnet was as follows:

$$F_{mag,NC1} = K_i i + K_{xe} x_e \quad (19)$$

The given voltage current equation of the proportional electromagnet was as follows:

$$U_g = \frac{1}{K_e} \left((R_L + K_e K_{fi}) i + L_h \frac{di}{dt} \right) \tag{20}$$

where K_i is the current-force gain coefficient of the proportional electromagnet, N/A; K_{xe} is the displacement-force gain coefficient of the proportional electromagnet, N/m. The value was very small: about 0. i is the current in the coil, A; x_e is armature displacement, m; R_L is the coil resistance and the internal resistance of the amplifier, Ω ; L_h is the coil inductance, H; K_e is the voltage amplification factor of the amplifier; and K_{fi} is the current feedback gain coefficient of the proportional electromagnet, V/A.

(3) Fluid flow system

For the simplified hydraulic system, the net volumetric flow rate to the NC1 actuator came from the flow rate exiting the safety valve, Q_{Line} . By applying the continuity equation at the safety valve exit, the flow rate at the inlet of the NC1, $Q_{NC1,X}$ and $Q_{NC1,in}$ were described by the following:

$$Q_{NC1,X} + Q_{NC1,in} = Q_{Line} - Q_{NC2} - Q_{NC3} - Q_{NC4} - Q_{NCF} - Q_{NCR} \tag{21}$$

where Q_{NC2} , Q_{NC3} , Q_{NC4} , Q_{NCF} , and Q_{NCR} are the flow rates to the proportional pressure reducing valves—NC2, NC3, NC4, NCF and NCR, respectively.

(a) Pilot valve

The flow through chamber X of the NC1 was defined by applying the following continuity equation to the chamber:

$$Q_{NC1,X,in} - Q_{NC1,X,ex} = \frac{V_{NC1,X}}{\beta} \frac{dP_{NC1,X}}{dt} \tag{22}$$

$$Q_{NC1, X\&C} = Q_{NC1,X,in} + Q_{NC1,C} \tag{23}$$

$$\begin{cases} Q_{NC1,X\&C} = C_d(\lambda) A'_{O11} \sqrt{\frac{2}{\rho} |\Delta P|} \text{sgn}(\Delta P) \\ \Delta P = P_{NC1,in} - P_{NC1,X} \end{cases} \tag{24}$$

where $Q_{NC1,X\&C}$ is the total flow rate into chambers X and C, m^3/s ; $C_d(\lambda)$ is the flow coefficient; A'_{O11} is the constant area of sharp-edged orifice 11, m^2 ; ρ is the density of the transmission fluid, kg/m^3 ; β is the transmission fluid bulk modulus, Pa; $Q_{NC1,X,ex}$ is the flow rate at the outlet of chamber X, m^3/s ; and $V_{NC1,X}$ is the volume of chamber X, m^3 .

(b) Main valve

The flow through chamber, B, of the NC1 was defined by applying the following continuity equation to the chamber, while the clutch was either filling or exhausting:

$$Q_{NC1,in} - Q_{NC1,control} = \frac{V_{NC1,B}}{\beta} \frac{dP_{NC1,B}}{dt} \tag{25}$$

$$Q_{NC1,control} - Q_{NC1,ex} = \frac{V_{NC1,B}}{\beta} \frac{dP_{NC1,B}}{dt} \tag{26}$$

where $V_{NC1,B}$ is the volume of chamber B, m^3 ; $P_{NC1,B}$ is the pressure in chamber B, Pa. $Q_{NC1,control}$ and $Q_{NC1,ex}$, are the metered flow rates at the output and the exhaust of NC1, respectively. The flow into and out of chambers A and

C was described by applying the continuity equation at those chambers. The resulting equations were given by the following:

$$Q_{NC1,A} + A_{NC1,A} \cdot \dot{x}_2 = \frac{V_{NC1,A}}{\beta} \frac{dP_{NC1,A}}{dt} \tag{27}$$

$$Q_{NC1,C} - A_{NC1,C} \cdot \dot{x}_2 = \frac{V_{NC1,C}}{\beta} \frac{dP_{NC1,C}}{dt} \tag{28}$$

$$\begin{cases} Q_{NC1,A} = C_d(\lambda) A'_{O12} \sqrt{\frac{2}{\rho} |\Delta P|} \text{sgn}(\Delta P) \\ \Delta P = P_{NC1,control} - P_{NC1,A} \end{cases} \tag{29}$$

where $Q_{NC1,A}$ and $Q_{NC1,C}$ are the flow rates into or out of chambers A and C, m^3/s ; \dot{x}_2 is the spool speed, m/s ; and $V_{NC1,A}$ and $V_{NC1,C}$ are the volumes in chambers A and C, m^3 .

Clutch Piston C1

The mathematical model of the clutch piston consists of two subsystems. They are the clutch piston mechanical dynamics and the fluid flow system.

(1) Clutch piston mechanical dynamics

The C1 piston motion depended on the pressure force acting on the piston, they were as follows: the spring force, the inertia force, and the viscous damping force. The static friction force and the flow force were assumed to be negligible. Thus, the mechanical dynamics of the C1 piston were described by the following:

$$m_{C1} \ddot{x}_{C1} + B_{C1} \dot{x}_{C1} + K_{C1} x_{C1} = A_{C1} P_{C1} - F_{initial,C1} \tag{30}$$

where m_{C1} is the mass of the clutch piston, kg ; B_{C1} is the viscous damping coefficient, $N/(m/s)$; K_{C1} is the spring constant, N/mm ; A_{C1} is the pressure acting area of the clutch piston, m^2 ; P_{C1} is the pressure applied to the clutch piston, Pa ; $F_{initial,C1}$ is the spring preload, and N ; x_{C1} , is defined as piston displacement and measured from the unloaded static equilibrium, m .

(2) Fluid flow system

The net volumetric flow rate to or from the clutch piston cavity, Q_{C1} , was determined by applying the continuity equation at the outlet of the clutch pressure regulation valve. Furthermore, Q_{C1} was also equal to the flow rate across accumulator #1. The resulting expression was given by the following equations:

$$Q_{C1} = Q_{NC1,control} - Q_{NC1,A} \tag{31}$$

$$\begin{cases} Q_{C1} = C_d(\lambda) A'_{O13} \sqrt{\frac{2}{\rho} |\Delta P|} \text{sgn}(\Delta P) \\ \Delta P = P_{NC1,control} - P_{C1} \end{cases} \tag{32}$$

The parameters used in the simulation of the hydraulic actuation system are summarized in Table 3.

Table 3. Parameters used in simulation of the hydraulic actuation system.

Parameter	Value	Parameter	Value
D_{pump} (cm^3/r)	30	KV_{PRV} ($m^3/s/Pa$)	8.33×10^{-7}
$P_{crack,PRV}$ (Pa)	2×10^6	m_1 (kg)	0.01
B_1 ($N/(m/s)$)	10	m_2 (kg)	0.04
B_2 ($N/(m/s)$)	100	K_{NC1} (N/mm)	10
$C_d(\lambda)$	0.7	ρ (kg/m^3)	850
β (Pa)	1.7×10^9	m_{C1} (kg)	0.5
B_{C1} ($N/(m/s)$)	200	K_{C1} (N/mm)	438
$F_{initial,C1}$ (N)	500	A_{C1} (m^2)	0.0217

3. Simulation Analysis of the Shift Process

3.1. Evaluation Indexes of Shift Quality

Acceptable jerk and shift time were selected as the evaluation indexes of shift quality.

3.1.1. Acceptable Jerk

The traditional calculation formula of jerk, that is, the derivative of acceleration, is as follows [18,19]:

$$J(t) = \frac{da}{dt} = \frac{d^2v}{dt^2} \quad (33)$$

The traditional calculation of jerk does not consider the influence of frequency and action time, so, this paper presented an evaluation index (acceptable jerk), which considered the effect of the two factors, peak jerk and root mean square jerk, as follows:

$$J_{ajv} = 0.004J_{max}^2 + J_{rms} \quad (34)$$

where J_{max} is the peak jerk, $J_{max} = \max(J(t))$, m/s^3 ; J_{rms} is the root mean square jerk, $J_{rms} = \sqrt{\frac{\int_0^{t_e} J^2(t)dt}{t_e}}$, m/s^3 ; t_e is the shift time, s.

3.1.2. Shift Time

Shift time is the time required after the steady state of the previous range changes to a new range. It is a comprehensive index, reflecting tractor shift quality. Good shift quality requires less shift time on the basis of a smooth shift. This paper held that the shift process was finished when the total torque capacity of the oncoming clutch reached 99% of the stable torque capacity.

3.2. Simulation Model of Powertrain

According to the design scheme of the HMCVT in Figure 1, the simulation model of the powertrain, based on AMESim, is shown in Figure 5. The simulation model mainly included the following four modules: the transmission module of the HMCVT, the hydraulic component actuation, the calculation module for evaluation indexes, and the rear axle and longitudinal tractor model. The transmission module of the HMCVT can be subdivided into the following three parts: the engine speed and tractive resistance of the tractor, the variable displacement pump-fixed displacement motor system, and the HMCVT mechanical system. All the clutches were controlled by the pilot-operated proportional pressure reducing valves. The calculation module for evaluation indexes was used to calculate the jerk of the HMCVT output shaft.

3.3. Continuous Shift Process of HMCVT

The simulation condition can be expressed as follows: $N_e = 2000$ r/min, $F_r = 5$ kN, $P_c = 2$ MPa, $D_o = 3.5$ mm. The whole continuous shift process included the upshift from range 1 to range 4 in the first 40 s, and the downshift from range 4 back to range 1 in the next 40 s. The simulation time of each range of the HMCVT was 10 s, the engagement states of the clutches were changed in the 0th second of each range (0 s, 10 s, 20 s, 30 s, 50 s, 60 s, and 70 s). The swash value of the variable displacement pump-fixed displacement motor system was changed in the last 5 s of each range (5–10 s, 15–20 s, 25–30 s, 35–40 s, 45–50 s, 55–60 s, 65–70 s, and 75–80 s). The simulation curves of the continuous shift process are shown in Figure 6.

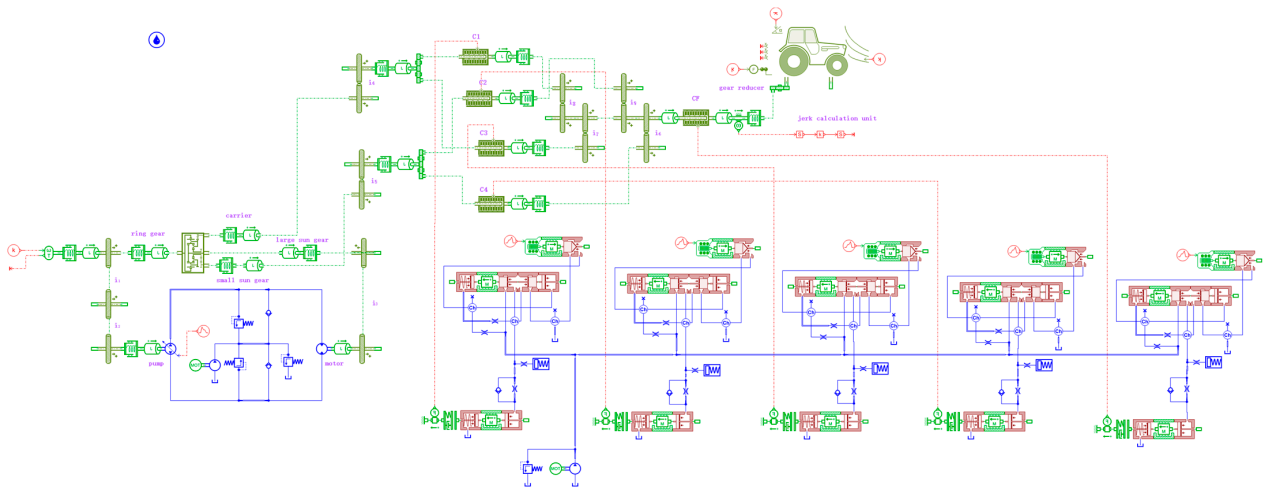


Figure 5. Powertrain simulation model.

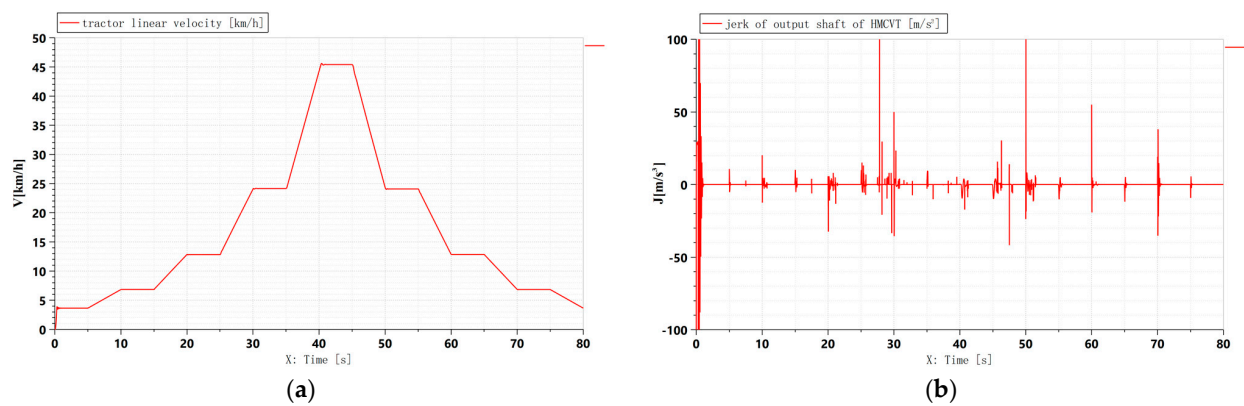


Figure 6. Simulation results of the continuous shift process of HMCVT. (a) Simulation result of the tractor linear velocity; (b) Simulation result of the jerk of the output shaft.

The simulation results showed that when the tractor's range changed, there was a slight fluctuation in the tractor's speed, and the jerk of the HMCVT output shaft was large. We can infer that the range switching from range 1 to range 4 are the typical operating conditions for improving the shift quality. The working speed of a tractor plowing is generally 5–10 km/h, while that of a tractor sowing is 6–15 km/h. In the whole working life cycle of tractors, the speed of 4–15 km/h accounts for about 75% [22]. As such, this paper took the range 1 to range 2 upshift to study the effect of tractor parameters on the shift quality.

3.4. Analysis on the Influence of Tractor Parameters on the Shift Quality (Range 1 to Range 2)

According to practical experience, the following factors may affect the shift quality: engine speed, the tractive resistance of the tractor, the clutch oil pressure, and the orifice diameter, etc. In this study, the engine speed was set at 1000–2000 r/min, and the range of the tractive resistance of the tractor was 5–20 kN. The range of clutch oil pressure was 1–2 MPa and the orifice diameter range was 2.5–3.75 mm. In the following tests, each parameter was further divided into six levels.

3.4.1. The Shift Process under the Influence of a Single Parameter

1. Engine speed

The simulation condition can be expressed as follows: $F_r = 5$ kN, $P_c = 2$ MPa, $D_o = 3.5$ mm. Six tests were conducted at engine speeds of 1000 r/min, 1200 r/min, 1400 r/min, 1600 r/min, 1800 r/min, and 2000 r/min. The test results are shown

in Figure 7a. In general, the acceptable jerk value increased with the engine speed during the shift process. The shift time decreased with the increase in engine speed, and did not change after 0.24 s. Therefore, the engine speed had a significant effect on the acceptable jerk and shift time.

2. Tractive resistance of the tractor

The simulation condition can be expressed as follows: $N_e = 2000$ r/min, $P_c = 2$ MPa, $D_o = 3.5$ mm. Six tests were conducted at the tractive resistances of the tractor of 5 kN, 8 kN, 11 kN, 14 kN, 17 kN, and 20 kN. The test results are shown in Figure 7b. The acceptable jerk value increased with the increase of the tractive resistances of the tractor during the shift process; the shift times were all 0.24 s. Therefore, the tractive resistance of the tractor had no effect on the shift time, but it had a significant effect on the acceptable jerk.

3. Clutch oil pressure

The simulation condition can be expressed as follows: $N_e = 2000$ r/min, $F_r = 5$ kN, $D_o = 3.5$ mm. Six tests were conducted at the clutch oil pressure of 2 MPa, 1.8 MPa, 1.6 MPa, 1.4 MPa, 1.2 MPa, and 1 MPa. The test results are shown in Figure 7c. The acceptable jerk value decreased with the decrease of clutch oil pressure during the shift process. The shift time varied with the change of the clutch oil pressure during the shift process, but it did not reflect the regularity. Therefore, the clutch oil pressure had an irregular impact on the shift time and had a significant impact on the acceptable jerk.

4. Orifice diameter

The simulation condition can be expressed as follows: $N_e = 2000$ r/min, $F_r = 5$ kN, $P_c = 2$ MPa. Six tests were conducted at the orifice diameters of 3.75 mm, 3.5 mm, 3.25 mm, 3 mm, 2.75 mm, and 2.5 mm. The test results are shown in Figure 7d. The acceptable jerk value decreased with the decrease of the orifice diameter, but if the orifice diameter was too small, it caused an increase in the acceptable jerk value. The shift time increased with the decrease of the orifice diameter. Therefore, the orifice diameter had a significant effect on the shift time and the acceptable jerk.

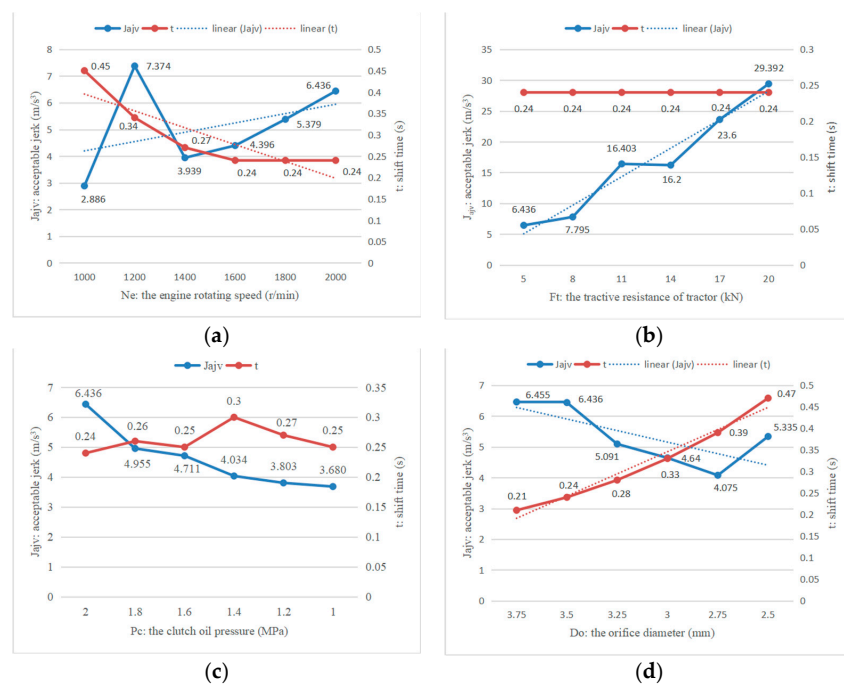


Figure 7. The test results of a single parameter. (a) The test results of the engine speed; (b) The test results of the tractive resistance of the tractor; (c) The test results of the clutch oil pressure; (d) The test results of the orifice diameter.

3.4.2. The Shift Process under the Influence of Combined Parameters

In practice, the shift process was affected by combined parameters. Therefore, uniform design experimentation could be used for the research [23]. The uniform design experimentation method was proposed by the Chinese mathematicians Fang, K.T. and Wang, Y. in 1978. It is a test method that only considers the uniform distribution of test points in the test range. The uniform design table was used to arrange the experiment, and the regression analysis method was used to analyze the experimental data. The uniform design experimentation method is especially suitable for occasions with a large range of variables and many levels of factors (if the number of levels is not less than five).

The level values of all the factors are shown in Table 2. Firstly, according to the number of factors and levels, we selected a uniform design table, $U_6^*(6^4)$ or $U_7(7^4)$ [24]. Next, according to their usage table, when the factor number (m) is four, the deviations of the two tables are 0.2990 and 0.4750, respectively. Finally, based on the principle of minimum deviation, the uniform design table, $U_6^*(6^4)$, was used for the test, and the test scheme is shown in Table 4.

Table 4. Design of shift test scheme influenced by multi-factor, $U_6^*(6^4)$.

Test	N_e : Engine Speed (r/min)	F_r : Tractive Resistance of Tractor (kN)	P_c : Clutch Oil Pressure (MPa)	D_o : Orifice Diameter (mm)	Observed Response Value y
1	1000(1)	8(2)	1.4(3)	3.75(6)	y1
2	1200(2)	14(4)	2(6)	3.5(5)	y2
3	1400(3)	20(6)	1.2(2)	3.25(4)	y3
4	1600(4)	5(1)	1.8(5)	3(3)	y4
5	1800(5)	11(3)	1(1)	2.75(2)	y5
6	2000(6)	17(5)	1.6(4)	2.5(1)	y6

The test results that were obtained according to this scheme are shown in Table 5. The analysis and processing of the test data will be presented later.

Table 5. The test results of acceptable jerk and shift time.

Test	N_e : (r/min)	F_r : (kN)	P_c : (MPa)	D_o : (mm)	J_{ajv} : (m/s ³)	t_e : (s)
1	1000(1)	8(2)	1.4(3)	3.75(6)	5.05	0.25
2	1200(2)	14(4)	2(6)	3.5(5)	11.44	0.34
3	1400(3)	20(6)	1.2(2)	3.25(4)	25.96	0.20
4	1600(4)	5(1)	1.8(5)	3(3)	3.82	0.28
5	1800(5)	11(3)	1(1)	2.75(2)	13.46	0.28
6	2000(6)	17(5)	1.6(4)	2.5(1)	19.23	0.41

3.4.3. The Influence of Combined Parameters on Acceptable Jerk

Firstly, the multiple linear regression model was used for the analysis and processing of the test data. Secondly, the stepwise regression method was selected to select the variables, and then the variable with the greatest contribution was selected for inclusion in the regression equation. Two pre-determined thresholds, F_{in} and F_{out} , were used to determine whether a variable should be selected or eliminated from the regression equation. Finally, the regression equation was as follows:

$$J_{ajv} = -4.842 + 1.440F_r \tag{35}$$

The value's residual standard deviation ($\hat{\sigma}^*$) and multi-correlation index (R^2) in the regression analysis were 2.741 and 0.916, respectively. Equation (35) shows that only one parameter, F_r , had a significant effect on J_{ajv} , while the other three parameters had no significant effect. This is not consistent with actual experience. Practical problems often

need to consider high-order interaction, so the linear model does not necessarily meet the requirements. Therefore, a quadratic regression model was proposed, as follows:

$$Y = \beta_0 + \sum_{i=1}^m \beta_i X_i + \sum_{i=1}^m \beta_{ii} X_i^2 + \sum_{i < j} \beta_{ij} X_i X_j + \varepsilon_0 \tag{36}$$

where $\beta_0, \beta_i, \beta_{ii}, \beta_{ij}$ are the regression coefficients; ε_0 is the random error. There are 15 terms in Equation (36). The regression equation can be obtained by using a stepwise regression technique, as follows:

$$J_{ajv} = 9.969 + 0.054F_r \times F_r - 0.14P_c \times D_o \tag{37}$$

The value's residual standard deviation ($\hat{\sigma}^*$) and multi-correlation index (R^2) in this regression analysis were 0.952 and 0.992, respectively, and $t_0 = 5.918, t_1 = 17.336, t_2 = -4.709$. Obviously, the effect of Equation (37), was better than Equation (35).

Equation (37) shows that: parameters, F_r , and interaction, $P_c \times D_o$, had significant effects on J_{ajv} , because $|t_1| > |t_2|$, so F_r was more important than $P_c \times D_o$. The larger the tractive resistance of the tractor, F_r , is, the more significant the impact on the acceptable jerk, J_{ajv} , is. The clutch oil pressure, P_c , and the orifice diameter, D_o , had a negative interaction with the acceptable jerk, J_{ajv} .

3.4.4. The Influence of Combined Parameters on Shift Time

The multiple linear regression model was used for the analysis and processing of the test data. Backward elimination was used to filter the variables. Firstly, all the variables were used to fit the regression equation, and then the variables that had no significant contribution to the equation were gradually eliminated, until all the variables in the equation had a significant contribution. The initial regression equation was as follows:

$$t_e = 0.386 + 0.001F_r + 0.013P_c - 0.097D_o \tag{38}$$

The next step was to conduct an analysis of variance on equation 38. The result is shown in Table 6.

Table 6. Analysis of variance table.

Source	Sum of Squares	df	Mean Square	F
Regression	0.018	3	0.006	1.328
Residual Error	0.009	2	0.004	
Total	0.027	5		

When $\alpha = 0.05$, the critical value, $F_{3,3}(0.05)$, of the F table is $9.23 > F = 1.328$, so equation 38 was not credible. After this, the variables that had the least significant contribution to the equation were removed in turn, and the regression analysis was carried out. Finally, it was found that there was no regression relationship between t_e and the four parameters (N_e, F_r, P_c, D_o). The test results showed that the four parameters (N_e, F_r, P_c, D_o) had no significant effect on the shift time, t_e .

3.5. Discussion

In previous studies, the indexes selected to evaluate the shift quality were transient indexes, chosen without considering the time process influence of shift jerk. Since shift is a continuous process, it is obviously unreasonable to only consider the transient maximum. In our research, the acceptable jerk and the shift time were selected as the evaluation indexes of shift quality. The acceptable jerk considered the effect of the two factors, peak jerk and root-mean-square jerk. The peak jerk refers to the maximum jerk during the shift. The jerk reflects the continuous impact of the jerk within the shift time. Therefore, the

evaluation indexes of this paper were more comprehensive than the evaluation indexes in previous studies.

Previous research that has been conducted [15,16] only studied the influence of a single design parameter on shift quality, and did not further explore the influence of combined parameters closer to the actual engineering situation. The research [18,19] studied the influence of combined parameters on shift quality by an orthogonal test method, but did not consider the interaction between combined parameters, and the level number of each parameter was too small (only three). In our research, the uniform design experimentation method was used to explore the comprehensive influence of multi-level combined parameters on tractor shift quality. We designed a uniform design table with four parameters and six levels, and the complete experimental design goal was completed after six tests. The complex relationship between the four parameters was obtained by using regression analysis. In the same case, 49 tests would have been required if the orthogonal test method had been used, and further consideration of the interactions between parameters would have made the number of tests even greater. The results showed that the orthogonal test method was not suitable to study the influence of multi-level combined parameters on shift quality. The uniform design experimentation method used in this paper could not only effectively complete the test, but could also accurately obtain the complex interaction between the combined parameters, with the help of regression analysis.

4. Conclusions

In this paper, the kinetic model of tractor powertrain matching the HMCVT was established, and the shift quality of the tractor was analyzed. The simulation result of the tractor's continuous shift process showed us that when shifting between adjacent ranges, the jerk produced is large. This played a decisive role in the shift quality of the tractor.

The test results of a single parameter showed that there was a positive correlation between the acceptable jerk and the four parameters (the engine speed, the tractive resistance of the tractor, the clutch oil pressure, and the orifice diameter). The higher the values of the four parameters, the higher the acceptable jerk value of the tractor. However, the shift time was only negatively correlated with the engine speed and the orifice diameter. The larger the engine speed and orifice diameter, the smaller the shift time.

The uniform design experimentation method was used to analyze the shift jerk and shift time of the tractor, under the influence of multiple combined parameters. The test data were processed by using regression analysis. The test results showed us that the influence degree of the combined parameters on the acceptable jerk degree in the process of shift was as follows: the tractive resistance of the tractor and the interaction between the clutch oil pressure and the orifice diameter. Furthermore, the four parameters had no significant effect on the shift time.

Author Contributions: Conceptualization, J.W. and C.X.; methodology, J.W. and C.X.; software, J.W. and J.C.; validation, J.W. and J.C.; formal analysis, J.W. and X.F.; data curation, J.W.; writing—original draft preparation, J.W. and X.F.; writing—review and editing, J.W. and X.F.; visualization, J.W. and J.C.; supervision, C.X.; project administration, C.X.; funding acquisition, C.X. All authors have read and agreed to the published version of the manuscript.

Funding: This research was funded by the Key Research and Development Plan Project of Jiangsu Province, grant number BE2018343.

Institutional Review Board Statement: Not applicable.

Informed Consent Statement: Not applicable.

Data Availability Statement: The data in this study can be requested from the corresponding author.

Conflicts of Interest: The authors declare no conflict of interest.

Nomenclature

Nomenclature

J	lumped inertia, $\text{kg}\cdot\text{m}^2$
ω	angular velocity, rad/s
T	torque, Nm
$i_1 \sim i_{12}$	gear ratios
D	displacement, cm^3/r
ε	swash, $-1 \leq \varepsilon \leq 1$
p_1	high side pressure value of the pump-motor system, Pa
p_2	low side pressure value of the pump-motor system, Pa
V_1	volume of fluid on the high-pressure side, m^3
β	oil bulk modulus, Pa
$astrib$	Stribeck constant (positive value), r/min
T_{dyn}	maximum transmittable torque during sliding, Nm
T_{stat}	maximum transmittable torque during stiction, Nm
ω_{rel}	relative velocity, rad/s
m_t	tractor mass, kg
R_{wr}	radius of driving wheel, m
ω_{wr}	speed of driving wheel, rad/s
T_{wr}	driving wheel torque, Nm
T_{tr}	road load torque, Nm
T_{brake}	wheel braking torque, Nm
Q	volumetric flow rate, m^3/s
P	Pressure, Pa
ω_e	engine speed, rad/s
KV_{PRV}	pressure relief valve gain, $\text{m}^3/\text{s}/\text{Pa}$
P_{line}	line pressure, Pa
$P_{crack,PRV}$	cracking pressure, Pa
m_1	mass of the plunger in pilot valve, kg
B_1	viscous damping coefficient in pilot valve, $\text{N}/(\text{m}/\text{s})$
x_1	spool displacement in pilot valve, m
$F_{mag, \dots}$	magnetic force acting on the spool, N
$F_{1,flow, \dots}$	net steady flow force acting on the spool in pilot valve, N
A	land cross-sectional areas, m^2
m_2	mass of the plunger in main valve, kg
B_2	viscous damping coefficient in main valve, $\text{N}/(\text{m}/\text{s})$
x_2, \dot{x}_2	spool displacement in main valve, m ; spool speed in main valve, m/s
K_{NC1}	spring constant, N/mm
$F_{2,flow, \dots}$	net steady flow force acting on the spool in main valve, N
K_i	current-force gain coefficient of the proportional electromagnet, N/A
i	current in the coil, A
K_{xe}	displacement-force gain coefficient of the proportional electromagnet, N/m
x_e	armature displacement, m
U_g	proportional electromagnet voltage, V
K_e	voltage amplification factor of the amplifier
R_L	coil resistance and the internal resistance of the amplifier, Ω
K_{fi}	current feedback gain coefficient of the proportional electromagnet, V/A
L_h	coil inductance, H
Q_{Line}	flow rate exiting the safety valve, m^3/s
$Q_{NC1,X\&C}$	total flow rate into chambers X and C of the NC1
$C_d(\lambda)$	flow coefficient
A'	constant area, m^2
ρ	density of the transmission fluid, kg/m^3
m_{C1}	mass of the clutch piston, kg
B_{C1}	viscous damping coefficient, $\text{Nm}/\text{rad/s}$
K_{C1}	spring constant, N/mm
A_{C1}	pressure acting area of the clutch piston, m^2

$F_{initial,C1}$	spring preload, N
$x_{C1}, \dot{x}_{C1}, \ddot{x}_{C1}$	piston displacement, m; piston speed, m/s; piston acceleration, m/s ²
$J(t), J_{max}, J_{rms}$	jerk, peak jerk, root mean square jerk, m/s ³
J_{ajv}	acceptable jerk, m/s ³
t_e	shift time, s
N_e	engine speed, r/min
F_r	tractive resistance of tractor, kN
P_c	clutch oil pressure, MPa
D_o	orifice diameter, mm
$y_1 \sim y_6$	Observed Response Value
$\beta_0, \beta_i, \beta_{ii}, \beta_{ij}$	regression coefficients
ϵ_0	random error
Subscripts	
1~5	shaft 1~shaft 5
$C_1 \sim C_4$	shifting clutches
CF	directional clutch
$s1$	large sun gear
$s2$	small sun gear
r	ring gear
c	carrier
P	variable displacement pump
M	fixed displacement motor
PRV	pressure relief valve
$NC1, NC2,$ $NC3, NC4,$ NCF, NCR	pilot-operated proportional pressure reducing valve
$NC1, X/A/B/C$	chambers X/A/B/C of the NC1
$NC1, in$	inlet of the NC1
$NC1, X, in/ex$	inlet or outlet of chamber X of the NC1
$O11, O12, O13$	sharp-edged orifice 11, 12, 13
$NC1, control$	control outlet of the NC1
$NC1, ex$	exhaust of the NC1

References

- Macor, A.; Rossetti, A. Optimization of hydro-mechanical power split transmissions. *Mech. Mach. Theory* **2011**, *46*, 1901–1919. [\[CrossRef\]](#)
- Macor, A.; Rossetti, A. Fuel consumption reduction in urban buses by using power split transmissions. *Energy Convers. Manag.* **2013**, *71*, 159–171. [\[CrossRef\]](#)
- Rossetti, A.; Macor, A. Multi-objective optimization of hydro-mechanical power split transmissions. *Mech. Mach. Theory* **2013**, *62*, 112–128. [\[CrossRef\]](#)
- Zsolt, F.; György, K. Power flows and efficiency analysis of out- and input coupled IVT. *Period. Polytech. Mech. Eng.* **2009**, *53*, 61.
- Shamshirband, S.; Petkovic, D.; Amini, A.; Anuar, N.B.; Nikolić, V.; Čojbašić, Ž.; Kiah, M.L.M.; Gani, A. Support vector regression methodology for wind turbine reaction torque prediction with power-split hydrostatic continuous variable transmission. *Energy* **2014**, *67*, 623–630. [\[CrossRef\]](#)
- Rotella, D.; Cammalleri, M. Power losses in power-split CVTs: A fast black-box approximate method. *Mech. Mach. Theory* **2018**, *128*, 528–543. [\[CrossRef\]](#)
- Tanelli, M.; Savaresi, S.M.; Manzoni, V.; Monizza, F.; Taroni, F.; Mangili, A. Estimating the maneuver quality of an automatic motion inverter for end-of-line tuning in agricultural tractors. *IFAC Proc. Vol.* **2008**, *41*, 10726–10731. [\[CrossRef\]](#)
- Park, Y.; Kim, S.; Kim, J. Analysis and verification of power transmission characteristics of the hydromechanical transmission for agricultural tractors. *J. Mech. Sci. Technol.* **2016**, *30*, 5063–5072. [\[CrossRef\]](#)
- Raikwar, S.; Tewari, V.K.; Mukhopadhyay, S.; Verma, C.R.; Rao, M.S. Simulation of components of a power shuttle transmission system for an agricultural tractor. *Comput. Electron. Agric.* **2015**, *114*, 114–124. [\[CrossRef\]](#)
- Hu, J.; Wei, C.; Yuan, S.; Jing, C. Characteristics on hydro-mechanical transmission in power shift process. *Chin. J. Mech. Eng.* **2009**, *22*, 50–56. [\[CrossRef\]](#)
- Linares, P.; Méndez, V.; Catalań, H. Design parameters for continuously variable power-split transmissions using planetaries with 3 active shafts. *J. Terramechanics* **2010**, *47*, 323–335. [\[CrossRef\]](#)
- Kim, J.; Kang, J.; Kim, Y.; Min, B.; Kim, H. Design of power split transmission: Design of dual mode power split transmission. *Int. J. Automot. Technol.* **2010**, *11*, 565–571. [\[CrossRef\]](#)

13. Cammalleri, M.; Rotella, D. Functional design of power-split CVTs: An uncoupled hierarchical optimized model. *Mech. Mach. Theory* **2017**, *116*, 294–309. [[CrossRef](#)]
14. Wang, J.; Xia, C.; Fan, X.; Cai, J. Research on transmission characteristics of hydromechanical continuously variable transmission of tractor. *Math. Probl. Eng.* **2020**, *2020*, 6978329. [[CrossRef](#)]
15. Kim, D.C.; Kim, K.U.; Park, Y.J.; Huh, J.Y. Analysis of shifting performance of power shuttle transmission. *J. Terramechanics* **2007**, *44*, 111–122. [[CrossRef](#)]
16. Wang, G.; Zhang, X.; Zhu, S.; Zhang, H.; Tai, J. Dynamic simulation on shift process of tractor hydraulic power split continuously variable transmission during acceleration. *Trans. Chin. Soc. Agric. Eng.* **2016**, *32*, 30–39.
17. Oh, J.Y.; Park, J.Y.; Cho, J.W.; Kim, J.G.; Kim, J.H.; Lee, G.H. Influence of a clutch control current profile to improve shift quality for a wheel loader automatic transmission. *Int. J. Precis. Eng. Manuf.* **2016**, *18*, 211–219. [[CrossRef](#)]
18. Zhu, Z.; Gao, X.; Pan, D.; Zhu, Y.; Cao, L. Study on the Control Strategy of Shifting Time Involving Multigroup Clutches. *Math. Probl. Eng.* **2016**, *2016*, 9523251. [[CrossRef](#)]
19. Zhu, Z.; Gao, X.; Cao, L.; Cai, Y.; Pan, D. Research on the shift strategy of HMCVT based on the physical parameters and shift time. *Appl. Math. Model.* **2016**, *40*, 6889–6907. [[CrossRef](#)]
20. Armstrong-HéLouvry, B. Control of machines with friction. *J. Tribol.* **1991**, *114*, 637. [[CrossRef](#)]
21. Watechagit, S. Modeling and Estimation for Stepped Automatic Transmission with Clutch-to-Clutch Shift Technology. Ph.D. Thesis, The Ohio State University, Columbus, OH, USA, 2004.
22. Ni, X. Study on Features of Multisession and Double Row Confluence Hydromechanical Continuously Variable Transmission of Tractor. Master's Thesis, Nanjing Agricultural University, Nanjing, China, 2013.
23. Fang, K.T. *Uniform Design and Uniform Design Table*, 1st ed.; Science Press: Beijing, China, 1994; pp. 38–50.
24. Zhuang, C.; He, C. *Fundamentals of Applied Mathematical Statistics*, 4th ed.; South China University of Technology Press: Guangzhou, China, 2013; pp. 387–398.